Computer Modeling of Planar Myocardial Perfusion Imaging: Effect of Heart Rate and Ejection Fraction on Wall Thickness and Chamber Size

Josef Machac, Howard Levin, Ethan Balk, and Steven F. Horowitz

Mount Sinai Medical Center, New York City, New York

Myocardial perfusion imaging is generally performed as a static acquisition without regard for dynamic changes in the cardiac cycle. The effect of heart rate and ejection fraction on the appearance of left ventricular chamber size and wall thickness as perceived in ^{201}Tl scintigrams has not, to our knowledge, been previously studied. A dynamic computer model of the left ventricle was constructed, capable of varying the heart rate and ejection fraction. Parallel slices through the model were convolved with experimentally derived ^{201}Tl point spread functions at corresponding depths to incorporate the effects of scatter and attenuation. Both gated and static left anterior oblique images were created at three clinically encountered heart rates and ejection fractions, with constant end-diastolic volume and left ventricular mass. Results of the study indicate that perceived and quantified wall thickness increases and chamber size decreases appreciably with increasing ejection fraction and (slightly) with increasing heart rate. Thus, evaluation of wall thickness and chamber size in planar images should take into account variations in heart rate and contractility. This is especially pertinent to estimates of left ventricular hypertrophy and chamber size, attempted from nongated myocardial perfusion images.

J Nucl Med 27:653–659, 1986

Planar myocardial perfusion imaging with thallium-201 (^{201}Tl) has been used for more than a decade as an important technique for the diagnosis of coronary artery disease. In addition to evaluating perfusion, a number of clinically relevant observations can be made from ^{201}Tl scintigrams concerning left ventricular chamber size and myocardial wall thickness. The finding of a dilated cavity or hypertrophied left ventricular myocardium conveys clinically relevant information. However, a number of theoretical factors may affect perceived cavity size and wall thickness in addition to true cavity dilatation and myocardial hypertrophy. These include attenuation, overlying structures, heart rate, and wall motion. The latter has been addressed previously with several authors finding that ECG gating of ^{201}Tl images decreases blurring due to wall motion (*1–5*). All investigators observed, as expected, that apparent wall thickness was greater and cavity size smaller on the composite views, compared with the gated end-diastolic views alone. Garty et al. (*5*) found thallium image gating to be advantageous for the detection of myocardial perfusion defects, although this was not supported by the findings of the other authors (*1–4*).

Thus, thallium imaging is routinely performed without gating, and the confounding influence of blurring due to wall motion remains unresolved. This has not been previously studied in a systematic fashion. We have designed a dynamic mathematic computer model that simulates the normal planar left ventricular myocardial perfusion image in order to examine the effect of different ejection fractions (EF) and heart rates (HR) on perceived wall thickness and chamber size on the composite, or "ungated" images.

MATERIALS AND METHODS

The overall method of modelling was similar to that of Vos et al. (*6*). The computer model of the myocardium consisted of a typical normal left ventricle with

Received Apr. 19, 1985; revision accepted Jan. 21, 1986.

For reprints contact: Josef Machac, MD, Annenberg 8, Mount Sinai Medical Center, One Gustave L. Levy Place, New York, NY 10029.

dimensions derived from routine two-dimensional echocardiograms and contrast ventriculography. The left ventricular diastolic myocardium was represented as 10 mm thick at the base and 5 mm thick at the apex in the shape of a parabola (Appendix 1) (*7*). The long axis of the inner volume was 10 cm from base to apex and the short axis 5 cm at the base (a 2.5-cm hemiaxis). This model was designed such that the inner volume could symmetrically decrease to any desired volume. The position of the base during the cycle was fixed. The dynamic ratio of long axis to short axis in diastole and systole was determined by a linear equation approximating the measurements obtained by Herman et al. (*8*) in their angiographic measurements (Appendix 2). These dimensions and their changes are also similar to measurements in normal subjects by Gould et al. (1974) (*9*). It was assumed that the uptake of thallium is uniform within the myocardium. The volume and mass of the myocardium and, therefore, the content of thallium within the myocardium were held constant throughout the cycle. This assumption was experimentally confirmed by Sanmarco and Davila (*10*) and utilized also in the work of Hugenholtz et al. (*11*) and Gould et al. (*9*). A typical gated blood-pool time-activity curve of a normal patient with an EF of 55% at a HR of 60 bpm was chosen as a reference in order to represent the volume change of the inner chamber throughout the cycle. The time-activity curve was also recorded at low levels of exercise at heart rates of 80 and 100 bpm. The EF for the model was controlled by scaling the time-activity curve to achieve EF of 30%, 55%, and 80% at each HR. The heart model was thus completely described mathematically.

The model could be projected in any desired orientation onto a three-dimensional matrix measuring 128 × 128 × 48 pixels with one cubic voxel measuring 0.23 cm, similar to the scale used in our routine clinical imaging. To facilitate the measurement of wall thickness and chamber size in this experiment, a symmetrical left anterior oblique (LAO) view was chosen. The heart model was rotated in the horizontal and vertical planes such that the long axis was perpendicular to the simulated Anger camera face. The tip of the ventricle in end-diastole was 2 cm deep to the surface of the "chest." For each of the 16 volumes within the cardiac cycle, 48 parallel slices of the model were manufactured from base to apex, along with background (*12*), and stored on flexible magnetic disks for later batch processing.

In order to simulate attenuation, scatter, and limited resolution of the collimator-Anger camera imaging system, the projected parallel slices of myocardial thallium at the various depths were convolved with the point spread functions of ^{201}Tl at the corresponding depths. This was accomplished by the following means. A thin (100λ) plastic pipette was suspended in a water bath. The shape of the bath was rectangular in order to obtain spatial uniformity. This thin pipette, 10 cm in length, was filled with a total of 200 mCi of thallous-201 chloride. This line source was then imaged with an Anger camera at progressive depths of 1 cm within the water bath starting at 1 cm up to a depth of 20 cm. The camera used for this experiment is employed for routine clinical thallium imaging and was equipped with a general all-purpose collimator. The images were stored in a 128 × 128 digital matrix. The profiles of the line spread functions then underwent discrete Fourier transformation in order to form a unidimensional filter (modulation transfer function). Filters corresponding to the exact depths of the 48 slices of the model were produced by linear interpolation between the 1-cm layers of acquired filters, starting at 2 cm, corresponding to the tip of the ventricle in end-diastole. A two-dimensional filter was formed by spinning the one-dimensional filter about the center of a 128 × 128 matrix, facilitated by an array processor. This operation assumes a two-dimensional symmetry of the imaging process. We confirmed this during the design process by comparing the line spread function of a horizontal and then a vertical source with the line spread function obtained from the inverse Fourier transform of the product of the Fourier transform of a hypothetically perfect line, and the two-dimensional filter, obtained from the same depth. The two techniques produced identical results, thus verifying the accuracy and validity of the convolution process. The two-dimensional Fourier transforms of the simulated myocardial sections at the various depths were multiplied by the appropriate two-dimensional filters and underwent an inverse Fourier transform, all performed by an array processor. This is equivalent to the convolution of the object model slices by the point spread functions at corresponding depths. These 48-layer images were then summed, producing the planar projection at one point in the cardiac cycle. Sixteen-frame image sets were manufactured for three different HR and three EFs. These sets were analogous to gated planar thallium images. The sum of the 16 frames of the cardiac cycle corresponded to static planar images. Figure 1 shows the simulated imaged ventricle in the typical anterior, LAO, and lateral views with a vertical tilt of 35°.

The apparent wall thickness and chamber size were evaluated both visually and quantitatively. Visual evaluation was performed by two experienced readers from computer displays of all nine assembled static LAO images at variable thresholds and contrast settings. Wall thickness and cavity size were compared across rows and down columns (Fig. 3) without knowledge of simulated EF or HR. The quantitative method employed measurements on a region of interest (ROI) identified by a uniform count threshold after background subtraction. Five arbitrary threshold levels were examined, the lowest demonstrating central cavity obliteration in

FIGURE 1
Example of simulated static anterior (45°), LAO (0°), and left lateral (−45°) views and moderate vertical tilt (35°)

at least one of the nine images. The highest threshold had the same count density as the peak counts in at least one of the nine images. This range fell between 84 and 100% of the peak counts of the image with the lowest peak counts. The measurements obtained were: the myocardial area (number of square pixels), the outer diameter, and the inner diameter of the left ventricular image measured in number of pixels. The wall thickness was one-half the difference between the outer and inner diameters.

RESULTS

Visual Assessment

Sample horizontal LAO gated images, together with the summed static images are shown in Fig. 2. The pair at the top shows the effect of changing the EF. The increased wall intensity and thickness and decreased chamber size in systole can be seen at the higher EF. The pair at the bottom of Fig. 2 shows the effect of a changing HR. Ventricular systole occurs later in the cycle and a larger fraction of time is spent in systole.

Figure 3 shows the nine static, summed images resulting from the combinations of the three EFs and three HRs. These images simulate static acquisitions of clinical studies in the LAO view for a horizontal heart. There was complete agreement in visual assessment of images between the two observers in noting the appearance of a smaller chamber and thicker myocardial wall at higher EFs. The change in left ventricular appearance with HR was slight. The difference was most apparent, however, at high EF, demonstrating a smaller chamber and thicker wall at higher HR.

Quantitative Measurements

The behavior of the area of the ROI, corresponding to the perceived myocardial mass, and characterized by an outer diameter, inner diameter, and wall thickness, were studied quantitatively for several fixed thresholds (Table 1). The myocardial area generally increased with higher HR and higher EF. Relatively greater changes were observed at higher thresholds. EF produced greater changes than the HR over the ranges of values studied. There were generally no changes in the outer diameter with either HR or EF manipulation (these results were not included in Table 1). The inner diameter consistently decreased at higher EF and decreased with a higher

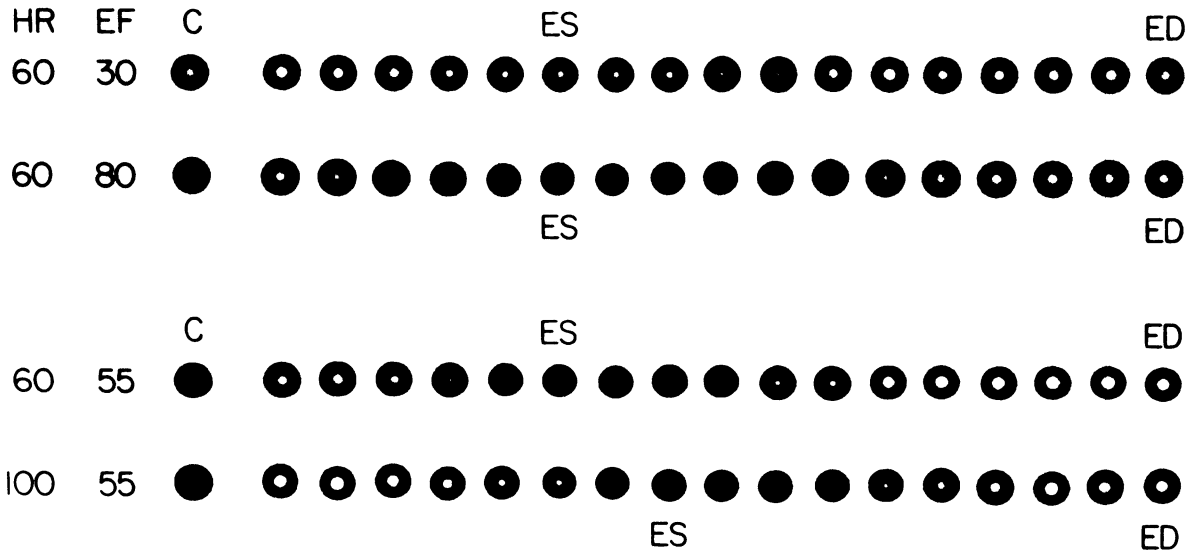

FIGURE 2
Examples of simulated gated ^{201}Tl left ventricular images in horizontal LAO view, and summed static views at extremes of EF, in %, and HR, in bpm. C = composite static view, ES = end systole, ED = end diastole

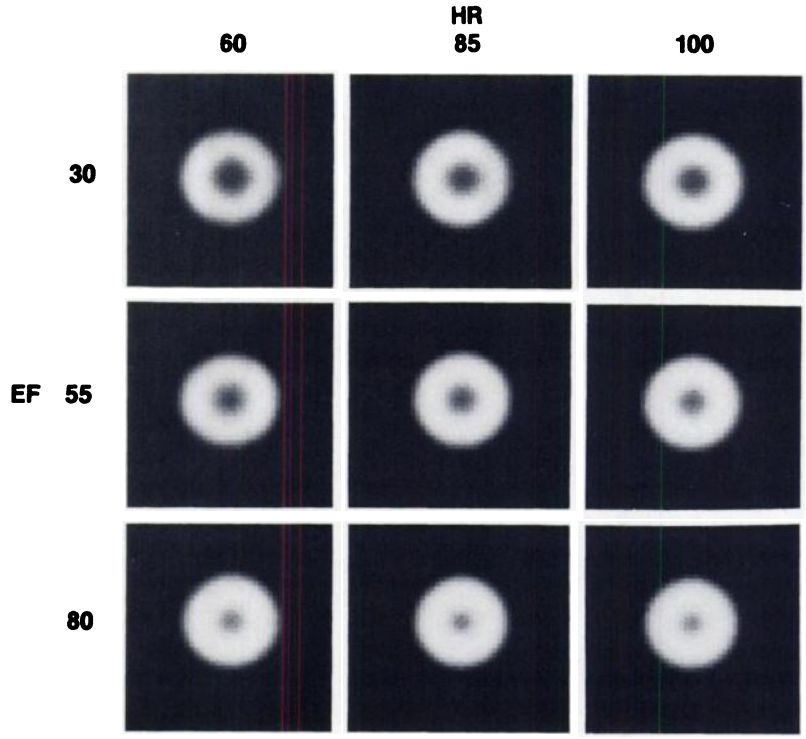

FIGURE 3
Simulated horizontal LAO views of same left ventricle at combinations of three values of HR, in bpm, and EF, in %

HR at some thresholds while remaining the same at others as seen in Table 1. Wall thickness was consistently increased at a higher EF, but increased slightly or remained constant with a higher HR.

DISCUSSION

The main purpose of the present study was to evaluate the influence of the cardiac cycle on perceived wall thickness and inner chamber size of the left ventricle as imaged by planar ^{201}Tl scintigraphy. Only one previous study, to our knowledge, has compared perception of left ventricular hypertrophy on planar ^{201}Tl images with two-dimensional, echocardiographic measurements (*13*). Although the effects of HR and wall motion on the myocardial perfusion image have been alluded to as a possible source of error in single photon emission computed tomography (SPECT)^{201}Tl mass measure-

TABLE 1
Left Ventricular Chamber Size, Wall Thickness, and Wall Area as Function of Heart Rate, Ejection Fraction, and % Threshold

		Threshold (% maximum)															
		81%			86%			90%			94%			98%		
Wall area (square pixels)																	
		HR			HR			HR			HR			HR		
		60	80	100	60	80	100	60	80	100	60	80	100	60	80	100
	30	256	256	264	218	220	222	176	180	180	132	152	160	64	92	96
EF	55	268	272	277	224	236	240	200	204	204	172	176	180	124	136	146
	80	272	280	280	228	240	242	216	220	228	180	196	200	148	156	164
Inner diameter (# pixels)																	
		60	80	100	60	80	100	60	80	100	60	80	100	60	80	100
	30	7	7	7	9	9	7	9	9	9	11	9	9	11	11	11
EF	55	5	5	5	7	5	5	7	7	7	9	7	7	9	9	9
	80	3	3	0	5	3	3	5	5	5	7	5	5	7	7	7
Wall thickness (# pixels)																	
		60	80	100	60	80	100	60	80	100	60	80	100	60	80	100
	30	6	6	6	5	5	6	4	4	4	3	4	4	2	2	2
EF	55	7	7	7	6	7	7	5	5	5	4	5	5	3	3	3
	80	8	8	9.5	6	7	7	6	6	6	5	6	6	4	4	4

ments (*14–16*), it has not yet been systematically studied nor considered in the single available clinical study (*13*).

HR and varying wall motion can, theoretically, affect the perceived planar images in a number of ways. A faster HR results in a greater proportion of time spent in systole when the ventricle is smaller and the myocardium thicker. A higher EF results in a smaller chamber volume and a thicker myocardium at all points of systole, although the time spent in systole is not significantly altered. On the other hand, a smaller mean chamber volume results in a greater distance between the ventricle and the detector, thus increasing the attenuation of the photons emanating from the myocardium and decreasing the relative attenuation difference between the base and the apex. Thus, the problem is spatially and temporally complex.

It would be difficult to explore the effects of HR and EF of the normal heart on the appearance of thallium images in vivo because of the difficulty inherent in precisely controlling such factors as myocardial thickness and contractility in humans or animals. A mathematic computer simulation was chosen over a mechanical model, since it proved to be extremely difficult to build and control a dynamic physical phantom with characteristics similar to the real heart (*17*). The computation time for the present model was greatly decreased by an array processor. This study is an example of the use of the array processor in applications other than SPECT reconstruction or routine smoothing operations.

The visual results show that there is a slight increase in count density and wall thickness with increasing HR, while at increasing EF there is a more easily appreciated, thicker myocardium and smaller chamber size, even though true myocardial mass remains the same. This finding suggests that assessment of left ventricular hypertrophy from nongated myocardial perfusion imaging is potentially misleading without knowledge of the state of myocardial contractility.

For purposes of quantitative comparison, the images in the present study were measured using variable, arbitrarily chosen thresholds. They were in the usable range of counts below which no central cavity would have been seen, and above which all myocardial activity would have been excluded. This range would be expected to vary from person to person depending on ventricular size and shape, amount of tissue scatter and camera resolution, as well as background uniformity. We chose the threshold method of edge detection, since this method would probably best approximate subjective visual assessment from film or computer console display, such as in Figs. 1, 2, and 3. The results of the quantitative measurements support the visual impressions.

At higher thresholds, the absolute and relative changes in the myocardial area, as a function of EF and HR, were greater. This may be due to the possible dominance of this region by the periapical segments, which recede away from the detector during systole. When the average distance from the detector is greater, as when the HR or EF are high, attenuation of activity causes a decrease in counts and, hence, a smaller profile. At a low threshold, the basal segments probably contribute more to the ROI, resulting in less sensitivity to the mean distance from the detector. This mechanism is complicated by changes in left ventricular geometry in systole. The variability in the presence or absence of a change in the measured dimensions of the inner chamber and wall thickness as a function of HR is undoubtedly due to the large size of the pixel relative to the magnitude of change measured, resulting in an all-or-none phenomenon. Although the pixel size is the same as used in our clinical work, the use of a finer matrix, in retrospect, would have been more helpful, although more tedious. Thus, these results should be viewed as a total impression from all thresholds. The changes in dimension measurements as a function of EF and changes in the measured area were more consistent, undoubtedly due to their greater magnitude, and thus less subject to the above sampling problem.

The dependence of the magnitude of changes in the measurement on the threshold value corresponds, in every day practice, to the effect of changing the exposure settings for film recording of images, or the manipulation of display parameters on computer screens. Thus, the visual impression of the effects of physiologic changes on the images is expected to be dependent on the display parameters. The problem appears unavoidable but it emphasizes the risk in such interpretations from images recorded on film where the threshold is arbitrarily set. In digital format, the observer can vary the display parameters to examine images as these under a variety of conditions. That is what we tried to do by selecting multiple thresholds to verify that measurements at one particular threshold were not unique. Although the magnitude of the changes in the measured parameters among the different thresholds differed, the patterns of change were similar. Thus the choice of threshold used would not alter the basic points of this study.

The range of EFs examined spans a wide spectrum of clinically encountered left ventricular function. The changes in HR between early and delayed thallium exercise studies usually lie within the range examined in this study. The change in EF between an early, postexercise study and delayed study would not be expected to be larger than 10–20%. However, the amount of change in EF that may occur in serial studies in a patient with a diffuse disease process could potentially be much greater. In viewing an ungated planar study of a particular patient for the first time, one does

not know whether the left ventricle looks thick because it is hypercontractile or hypertrophied.

The present work also has implications for three-dimensional imaging of the heart with ^{201}Tl SPECT, or positron emission tomographic (PET) imaging using any number of myocardial perfusion or metabolic tracers in which left ventricular mass can be quantified (*14–16*). An advantage of three-dimensional imaging lies in the ability to directly compare the measured mass with independent measurements using other invasive or noninvasive techniques (*11,14–16,18*). These three-dimensional methods, however, are also dependent on some method of myocardial edge detection, such as threshold, maximum gradient detection, or fitting to a model (*19*).

Regardless of the method of three-dimensional imaging and reconstruction, cardiac motion will remain as a problem for mass measurements. Since ^{201}Tl imaging suffers from a relatively low counting rate, gating in SPECT would be expected to be even less attractive than in planar images. However, the high count rates of PET using short-lived positron emitting isotopes has made the acquisition of gated images in a short time feasible, thus minimizing the effect of cardiac motion (*20*). Our model may be adapted for simulation of SPECT imaging to specifically study the effect of wall motion on measured left ventricular mass. Since PET imaging utilizes an entirely different concept of image data acquisition, a different model of simulation would need to be constructed, to deal with problems unique to PET such as different in-plane and out-of-plane sensitivities (*21*).

The present model makes a number of assumptions. We have chosen one typical ventricular shape and size. Similar, although not necessarily identical results would be expected for other ventricular shapes. We have assumed a uniform scattering medium similar to water, although the true chest tissues consist of a nonuniform composite ranging from air to bone, with a superimposed nonuniform background. Previous work has shown water to be a close approximation, providing satisfactory results for left ventricular volume measurements (*22,23*). This model examined only symmetric wall motion. Translational and rotational motion, frequently observed in gated cardiac blood-pool imaging, may account for some of the commonly found asymmetry between septal and posterolateral wall thickness on ^{201}Tl static images. It is also possible that this asymmetry is related to normally occurring regional differences in wall motion.

We conclude that the evaluation of chamber size and wall thickness from planar thallium images must be done with caution. The appearance of these images is significantly dependent on the EF, and, to a lesser extent, on HR. This may be of importance in interpreting studies in patients with hyperkinetic hearts (especially those immediately postexercise) and is influenced by the wide range of recovery time necessary for the heart rate to return towards baseline after stress. This observation has implications for measurements of myocardial mass and thickness in nongated ^{201}Tl SPECT and PET, suggesting the need for similar computer simulations in addition to standard clinical investigations.

ACKNOWLEDGMENT

This work was supported in part by Bernard and Josephine Chaus through the Heart Research Foundation.

APPENDIX 1

The equation of the inner and outer boundaries of left ventricle is:

$$Y = K \times SA^2,$$

where Y is the position along the long axis, SA is the radius or short axis at position Y, and K is a constant unique to the inner or outer surface.

APPENDIX 2

During the cardiac cycle, for a predetermined EF, the inner volume V_I follows a time-activity curve as described in the methods section, starting from an end-diastolic volume V_D. The short axis (SA), the long axis (LA), the basal thickness (BT) and apical thickness (AT) follow the following relationships:

$$\frac{\%\ \text{SA shortening}}{\%\ \text{LA shortening}} = 1.6$$

$$V_I = \frac{\pi(SA)^2 LA}{2}$$

$$AT = \frac{BT}{2}.$$

The outer volume (V_o) = $V_I + \Delta V$, where ΔV (total myocardial volume) is constant throughout the cycle. These equations determine the exact left ventricular size and shape.

REFERENCES

1. Planiol T, Itti R, Pellois A, et al: Dynamic cardiac scintigraphy with a multi-imaging device. *Eur J Nucl Med* 1:187–191, 1976
2. Hamilton GW, Narahara KA, Trobaugh GB, et al: Thallium-201 myocardial imaging: Characterization of the ECG-synchronized images. *J Nucl Med* 19: 1103–1110, 1978
3. Alderson PO, Wagner HN, Gomez-Moeiras JJ, et al: Simultaneous detection of myocardial perfusion and wall motion abnormalities by cinematic ^{201}Tl imaging. *Radiology* 127:531–533, 1978
4. McKillop JH, Fawcett HD, Boumert JE, et al: ECG gating of thallium-201 myocardial images: Effect on

detection of ischemic heart disease. *J Nucl Med* 22:219–225, 1981
5. Garty I, Kardontchik A: Study of ECG-gated thallium-201 myocardial scintigraphy: Is imaging time a limiting factor. *Eur J Nucl Med* 9:173–176, 1984
6. Vos PH, Vossepoel AM, Hermans JO, et al: Detection of lesions in thallium-201 myocardial perfusion scintigraphy. *Eur J Nucl Med* 7:174–180, 1982
7. Edwards WD, Tajik AJ, Seward JB: Standardized nomenclature and anatomical basis for regional tomographic analysis of the heart. *Mayo Clin Proc* 56:479–497, 1981
8. Herman MV, Heinle RA, Klein MD, et al: Localized disorders in myocardial contraction: Asynergy and its role in congestive heart failure. *N Eng J Med* 277:222–232, 1967
9. Gould KL, Lipscomb K, Hamilton GW, et al: Relation of left ventricular shape, function and wall stress in man. *Am J Cardiol* 36:627–634, 1974
10. Sanmarco ME, Davila JC: Continuous measurement of left ventricular volume in dogs: Estimation of volume-dependent variables using the ellipsoid model. In *Factors Influencing Myocardial Contractility*, Tanz RA, Kavaler F, Roberts J, eds. New York, Academic Press, 1967, p 199
11. Hugenholtz PG, Kaplan E, Hull E: Determination of left ventricular wall thickness by angiocardiography. *Am Heart J* 78:513–522, 1969
12. Narahara KA, Hamilton GW, Williams DL, et al: Myocardial imaging with thallium-201: An experimental model for analysis of the true myocardial and background image components. *J Nucl Med* 277:781–786, 1977
13. Bulkely BH, Rouleau J, Strauss HW, et al: Idiopathic hypertrophic subaortic stenosis detection by thallium-201 myocardial perfusion imaging. *N Eng J Med* 293:1113–1116, 1975
14. Holman BL, Moore SC, Sholkin PM, et al: Quantitation of perfused myocardial mass using Tl-201 and emission computed tomography. *Invest Radiol* 18:322–326, 1983
15. Wolfe CL, Corbett JR, Lewis SE, et al: Determination of left ventricular mass by single photon emission computed tomography with thallium-201. *Am J Cardiol* 53:1365–1368, 1984
16. Suzuki Y, Kadota K, Nohara R, et al: Recognition of regional hypertrophic cardiomyopathy using thallium-201 emission computed tomography: Comparison with two-dimensional echocardiography. *Am J Cardiol* 53:1095–1102, 1984
17. Horowitz SF, Miceli K, Blake T, et al: Effect of varying wall motion and thickness on detecting of non-transmural myocardial perfusion defects evaluated by a gated thallium-201 phantom. *Clin Res* 28:181A, 1980 (abstr)
18. Gould KL, Kennedy JW, Frimer M, et al: Analysis of wall dynamics and directional components of left ventricular contraction in man. *Am J Cardiol* 38:322–331, 1976
19. Kehtamavaz N, Philippe EA, DeFigueiredo RJP: A novel surface reconstruction and display method for cardiac PET imaging. In *IEEE Transactions on Medical Imaging*, Vol. MI-3, 1984, pp 108–115
20. Mullani NA, Gaeta J, Yerian K, et al: Dynamic imaging with high resolution time-of-flight PET camera—TOFPET I. In *IEEE Transactions on Nuclear Science*, Vol. NS-31, 1984, pp 609–613
21. Senda M, Yonekura Y, Tamakin N, et al: Axial resolution and the value of interpolating scan in multislice positron computed tomography. *J Nucl Med* 26:P28, 1985 (abstr)
22. Links JM, Becker LC, Shindledecker JG, et al: Measurement of absolute left ventricular volume from gated blood pool studies. *Circulation* 61:81–91, 1982
23. Starling M, Dell'Italia LJ, Nusynowitz ML: Estimates of left ventricular volumes by equilibrium radionuclide angiography: Importance of attenuation correction. *J Nucl Med* 25:14–20, 1984